Journal of Biomechanical Engineering. Received June 03, 2019;
Accepted manuscript posted January 1, 2020. doi:10.1115/1.4045812

Bond Graph Modeling of Mechanical Circulatory Support (MCS) Device - Cardiovascular System Interactions

Mengtang Li
Department of Mechanical Engineering
Vanderbilt University
2301 Vanderbilt Place, Nashville, TN 37235
Email: mengtang.li@vanderbilt.edu

Marvin J. Slepian
Department of Biomedical Engineering
Department of Medicine
Sarver Heart Center
University of Arizona
1501 N Campbell Ave, Tucson, AZ 85724
Email: chairman.syns@gmail.com

Eric J. Barth
Department of Mechanical Engineering
Vanderbilt University
2301 Vanderbilt Place, Nashville, TN 37235
Email: eric.j.barth@vanderbilt.edu

Abstract. *Though mechanical circulatory support (MCS) devices, such as ventricular assist devices (VAD) and total artificial hearts (TAH), provide heart failure patients with bridges to heart transplantation or are alternatives to transplantation, device performance and corresponding control strategies are often difficult to evaluate. Difficulties arise due to the complex interaction of multiple domains – i.e. biological, hydraulic, hemodynamics, electromechanical, system dynamics, and controls. In an attempt to organize, integrate and clarify these interactions, a technique often used in hydraulic pump design and robotics, called "bond graph modeling," is applied to describe the performance and functionality of MCS devices and the interaction between the cardiovascular system and the MCS device.*

This technical brief demonstrates the advantages of this tool in formulating a model for the systemic circulation interacting with the left side of a TAH, adopting the fundamental structure of either a hydraulic mechanism (i.e. AbioCor/Carmat) or a pneumatic mechanism (i.e. SynCardia), combined with a systemic circulation loop. The model captures the dynamics of the membrane, the hydraulic source or pneumatic source, and the systemic circulation. This multidisciplinary cross-pollination of an analytical tool from the field of dynamic systems may provide important insight to further aid and improve the design and control of future MCS systems.

1 Introduction

A "bond graph" is a graphical modeling method to describe the energy relationship within any physical dynamic system [1, 2]. Although seemingly similar to a block diagram or a signal flow graph, a bond graph mainly represents bi-directional energy exchange flows, instead of unidirectional information flows. Energy ports are linked via bonds. The energy flow within each bond is denoted by a pair of power variables called "effort" and "flow," over all connected bonds is the same while the flows sum to zero, and 1-junctions, where the flow through all connected bonds is the same while the efforts sum to zero. A unified model can be derived for multi-energy-domain systems using this method. Another significant feature of a bond graph is the causality, which indicates the feasibility of mathematical relationships in the real world. One dominant power variable (e.g. voltage) eventually specifies the other one (e.g. current), with the whole system energy exchange mechanism known (e.g. impedance). The effort and flow variables form a "handshake" mechanism between dynamic elements. In this manner, bond graphs allow modeling of subsystems with a first-principles mechanism of interaction with connected subsystems. Even though the cardiovascular system and an MCS device are very different, the bond graph methodology allows us to study their multi-energy-domain interaction.

2 Modeling

Research has been done to develop accurate models for the human circulation, including systemic and pulmonary circulations [3–7] and on the inter-dependence between the two sides [8]. Using a bond graph representation, such models can be paired with models of MCS devices to study their interactions [9, 10]. To illustrate the bond graph technique,

using a model similar to the cardiovascular system as described in [7], the interaction of the systemic circulation with one side of a TAH system is considered here. Distinct pressure locations are marked with 0-junctions and connected with cardiovascular elements through 1-junctions, as shown in Fig. 1a and Fig. 1b. The bond graph energy bonds (purple line with half arrow and end bar) were then obtained and marked by numbers. Due to four different modes of these two valves, three different cardiac phases, i.e. ejection phase, injection phase and isovolumetric phase, exist. Considering that only passive valves are used in currently available TAHs (Syncardia), such as the FDA approved rotating disk valve [11], the isovolumetric phase is not modeled here for the systemic circulation combined with a TAH.

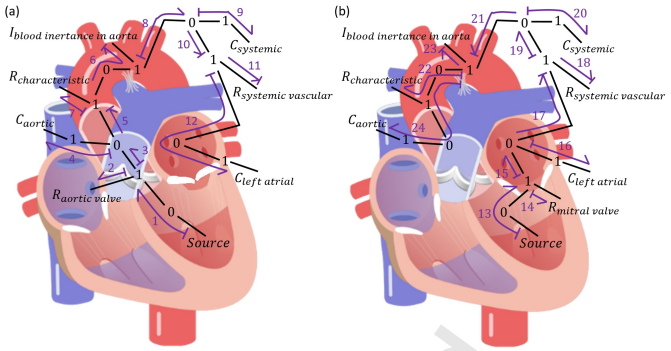

Fig. 1. (a) Bond graph graphic modeling of ejection phase (b) Bond graph graphic modeling of injection phase.

2.1 Ejection Phase Modeling

During the ejection phase, the aortic valve is open while the mitral valve is closed. The bond graph equations Eqns. (1-17) are derived below. The left atrial pressure (LAP), arterial pressure (AP), aortic pressure (AoP), aortic flowrate and outlet flowrate from the TAH are e_{12}, e_9, e_4, f_6 and f_1 respectively.

$$f_1 = f_2 = f_3 \tag{1}$$
$$e_1 = e_2 + e_3 \tag{2}$$
$$e_2 = R_3 f_2 \tag{3}$$
$$e_3 = e_4 = e_5 \tag{4}$$
$$f_3 = f_4 + f_5 \tag{5}$$
$$\dot{e}_4 = (1/C_4) f_4 \tag{6}$$
$$f_5 = f_6 = f_7 = f_8 \tag{7}$$
$$e_5 = e_6 + e_7 + e_8 \tag{8}$$
$$\dot{f}_6 = (1/I) e_6 \tag{9}$$
$$e_7 = R_4 f_7 \tag{10}$$
$$e_8 = e_9 = e_{10} \tag{11}$$
$$f_8 = f_9 + f_{10} \tag{12}$$
$$\dot{e}_9 = (1/C_3) f_9 \tag{13}$$
$$f_{10} = f_{11} = f_{12} \tag{14}$$
$$e_{10} = e_{11} + e_{12} \tag{15}$$
$$e_{11} = R_1 f_{11} \tag{16}$$
$$\dot{e}_{12} = (1/C_2) f_{12} \tag{17}$$

2.2 Injection Phase Modeling

During the injection phase, the aortic valve is closed while the mitral valve is open. The bond graph model equations Eqns. (18-34) are derived below. The LAP, AP, AoP, aortic flowrate and inlet flowrate from TAH are e_{16}, e_{20}, e_{24}, f_{23} and f_{13} respectively.

$$f_{13} = f_{14} = f_{15} \tag{18}$$
$$e_{13} = f_{14} + f_{15} \tag{19}$$
$$e_{14} = R_2 f_{14} \tag{20}$$
$$e_{15} = e_{16} = e_{17} \tag{21}$$
$$f_{15} = f_{16} + f_{17} \tag{22}$$
$$\dot{e}_{16} = (1/C_2) f_{16} \tag{23}$$
$$f_{17} = f_{18} = f_{19} \tag{24}$$
$$e_{17} = e_{18} + e_{19} \tag{25}$$
$$e_{18} = R_1 f_{18} \tag{26}$$
$$e_{19} = e_{20} = e_{21} \tag{27}$$
$$f_{19} = f_{20} + f_{21} \tag{28}$$
$$\dot{e}_{20} = (1/C_3) f_{20} \tag{29}$$
$$f_{21} = f_{22} = f_{23} = f_{24} \tag{30}$$
$$e_{21} = e_{22} + e_{23} + e_{24} \tag{31}$$
$$e_{22} = R_4 f_{22} \tag{32}$$
$$\dot{f}_{23} = (1/I) e_{23} \tag{33}$$
$$\dot{e}_{24} = (1/C_4) f_{24} \tag{34}$$

2.3 Hydraulic-Based TAH Modeling

A self-contained implantable MCS device, the Carmat TAH, consists of two independent ventricles separated by membranes into compartments for blood and hydraulic oil, four tricuspid valves for uni-direction flow, internal battery and transcutaneous energy transfer coils, as shown in Fig. 2a. Two external gear pumps are placed below the two ventricles and rotate back and forth to pump hydraulic oil to move the membranes, thus creating a pulsatile blood flow [12]. The fundamental pumping mechanism of the Carmat TAH can be modeled as a mass-spring-damper system powered by a controllable flow source, as in Fig. 2b. The elastic membrane is considered as a solid piston while its elasticity is modeled by spring stiffness and damping. The simplified bond graph model is shown in Fig. 2c and corresponding equations (35-46) are derived below.

Journal of Biomechanical Engineering. Received June 03, 2019;
Accepted manuscript posted January 1, 2020. doi:10.1115/1.4045812

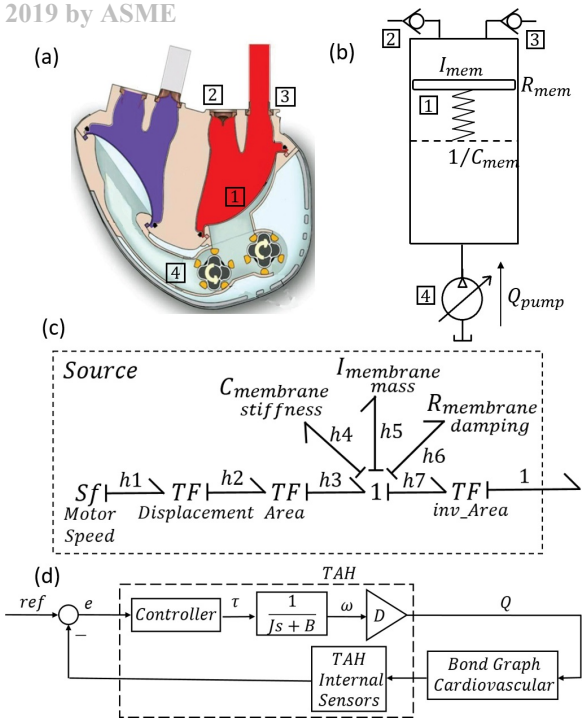

Fig. 2. (a) Cross-sectional view of Carmat TAH: ①membrane, ②inlet valve, ③outlet valve, ④gear pumps (b) Simplified dynamic model of Carmat TAH (c) Bond graph of Carmat TAH (d) Control block diagram

$$f_{h1} = S_f \tag{35}$$
$$f_{h2} = Df_{h1} \tag{36}$$
$$e_{h1} = De_{h2} \tag{37}$$
$$f_{h3} = (1/A_{mem})f_{h2} \tag{38}$$
$$e_{h2} = (1/A_{mem})e_{h3} \tag{39}$$
$$f_{h3} = f_{h4} = f_{h5} = f_{h6} = f_{h7} \tag{40}$$
$$e_{h3} = e_{h4} + e_{h5} + e_{h6} + e_{h7} \tag{41}$$
$$\dot{e}_{h4} = (1/C_{mem})f_{h4} \tag{42}$$
$$\dot{f}_{h5} = (1/I_{mem})e_{h5} \tag{43}$$
$$e_{h6} = R_{mem}f_{h6} \tag{44}$$
$$f_1 = A_{mem}f_{h7} \tag{45}$$
$$e_{h7} = A_{mem}e_1 \tag{46}$$

With 16 unknowns but only 15 equations, the following restriction or relation can be obtained.

$$f_1 = DS_f \tag{47}$$

which means the flowrate of the hydraulic pump determines the flowrate of the TAH directly without the effect of the cardiovascular system. Once the driving signal, pump speed $S_f = f_{h1}$, is given, the equation set is solvable and the interaction between the TAH and the circulation system can be simulated and analyzed.

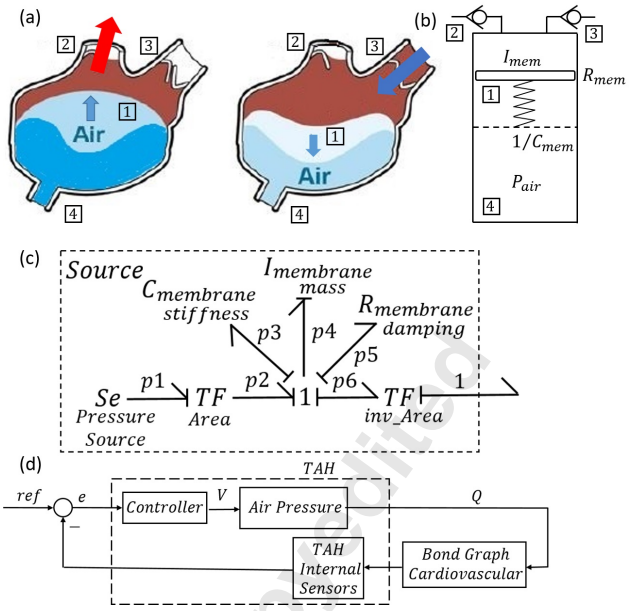

Fig. 3. (a) Cross view of SynCardia TAH: ①membrane, ②outlet valve, ③inlet valve, ④ external pressure source (b) Simplified dynamic model of SynCardia TAH (c) Bond graph model of SynCardia TAH (d) Control block diagram

2.4 Pneumatic Based TAH Modeling

As the only FDA approved TAH for use as a bridge to transplantation (2004) and for long-term (destination) implantation (2012), the SynCardia heart, shown in Fig. 3a, is composed of two independent polyurethane ventricles with 70 mL volume, four mechanical valves for uni-directional flow control, and two percutaneous pneumatic tubes for connecting to the external console. Blood inflow and ejection motion is realized by the membranes which are controlled by a pneumatic pressure differential across the membranes. The dynamic mechanism of the membrane can be modeled as a mass-spring-damper system powered by a controllable pressure source, as in Fig. 3b. The semi-elastic membrane is considered as a solid piston while its elasticity is modeled by spring stiffness and damping. The simplified bond graph model is shown in Fig. 3c. As mathematically proven in Eqn. (47) previously, the TAH flowrate equals that of the source. While for the hydraulic based TAH, such as the Carmat or AbioCor, the source flow is known (specified by the controlled motor speed), for the pneumatic based TAH, such as SynCardia, the flow from the source is unknown and it depends on the interaction with the rest of the cardiovascular system (pressure is the specified effort source).

The dynamic model of the pneumatic power mass-spring-damper system is described as follows

$$f_1 = f_{p1} \tag{48}$$
$$I_{mem}\ddot{f}_{p2} = A_{mem}(e_{p1} - e_1) - R_{mem}\dot{f}_{p2} - C_{mem}f_{p2} \tag{49}$$
$$f_1 = Af_{p2} \tag{50}$$
$$e_1 = \begin{cases} AoP + R_3 f_1 & \text{, if } f_1 > 0 \\ LAP + R_2 f_1 & \text{, if } f_1 < 0 \end{cases} \tag{51}$$

Once the driving signal, air pressure $S_e = e_{p1}$, is given, the equation set is solvable and the interaction between the TAH and the circulation system can be simulated and analyzed.

3 Results

Various methods and tools exist to solve the bond graph model. Our results demonstrate that the model can be utilized to investigate the effects of either varying CV conditions encoded by the model's parameters (e.g. afterload) or altering mechanical properties of the TAH (e.g. damping, moment of inertia of the pump rotor, or stiffness of the pneumatic membrane). Such investigation is useful in evaluating a particular design and thereby guide and improve any model-guided design iteration. The hydraulic and pneumatic based TAHs are controlled to track a cardiac output and flowrate emulating a human heart [13], with the associated control block diagram shown in Fig. 2d and Fig. 3d respectively.

Bond graph model parameters for the systemic circulation [14] and hydraulic and pneumatic based TAHs are listed in Tab. 1. To ensure the correctness and consistency of the modeling from the energy point of view, SI units are used and then converted into medical standard units.

3.1 Hydraulic Based TAH + Circulation

The hemodynamics of the hydraulic based TAH circulation system under four different afterload operating conditions are shown in Fig. 4. As the afterload increases, higher LVP is required to open aortic valve to eject blood into aorta. The delayed valve open time and decreased blood pumping effects are also noticeable from Fig. 4a and 4b. Note that compared with the native heart, the blood pumping chamber of this hydraulic based TAH is smaller (to fit the entire device in a patient's chest), which leads the end systolic pressure volume relationship (ESPVR) in Fig. 4c intersects with horizontal axis at a different location.

3.2 Pneumatic Based TAH + Circulation

Unlike the hydraulic-based TAH, the control strategy for a pneumatic-based TAH is more complex. Figure 5 plots the hemodynamics of the pneumatic based TAH circulation system under four different afterload operating conditions. Reduced pressure required to open aortic valve, delayed valve opening time and decreased amount of pumping blood due to increased afterload pressure can be seen from Fig. 5. Also, compared with the native heart, the blood pumping chamber of a pneumatic based TAH (e.g. 70 mL for SynCardia) is smaller in size to fit within the patient's chest. The consequence of this smaller size, at least for this control algorithm, is that it cannot comply with the ESPVR once it reaches the volume limits, as the blue PV-loop shown in Fig. 5c.

4 Conclusions

The net performance of implanted MCS devices involves the balance of interaction between the device and the overall cardiovascular system of the individual patient into whom it is implanted. Bond graph modeling provides a quantitative methodology for universally describing a complex system containing subsystems from the perspective of differing energy domains. This technical brief highlights this methodology to suggest its value, and offer it as a tool to further understand MCS-human CV system interactions, as well as to examine the behavior of parameters and variables which may be optimized to enhance device and system design. This approach adds an additional tool to the cardiovascular biomechanical engineer, physiologist and physician with potential for enhancing the safety and efficacy of MCS systems, thereby reducing adverse events and improving their clinical utility.

5 Limitations

Here we present only a simple bond graph model describing the interaction between the systemic circulation loop with the left side of a basic TAH. A more detailed model is needed to take into account the right (pulmonary) side of the heart and interdependence between left and right sides, isovolumetric phase, and the dynamics of heart valves. What we present is a starting point, as ultimately further model validation will be needed. Finally, we must keep in mind that the traditional bond graph technique utilizes SI units during calculation, resulting in un-common medical standard units.

Acknowledgements

We acknowledge support for the Arizona Center for Accelerated Biomedical Innovation (ACABI) of the University of Arizona.

References

[1] Paynter, H. M., 1961. *Analysis and design of engineering systems*. MIT press.

[2] Karnopp, D., and Rosenberg, R. C., 1968. "Analysis and simulation of multiport systems: The bond graph approach to physical system dynamics".

[3] Bai, J., Ying, K., and Jaron, D., 1992. "Cardiovascular responses to external counterpulsation: a computer simulation". *Medical and Biological Engineering and Computing,* **30**(3), pp. 317–323.

[4] De Lazzari, C., Ferrari, G., Mimmo, R., Tosti, G., and Ambrosi, D., 1994. "A desk-top computer model of the circulatory system for heart assistance simulation: effect of an lvad on energetic relationships inside the left ventricle". *Medical engineering & physics,* **16**(2), pp. 97–103.

[5] Xu, L., and Fu, M., 2000. "Computer modeling of interactions of an electric motor, circulatory system, and rotary blood pump". *ASAIO journal,* **46**(5), pp. 604–611.

Table 1. Bond graph model parameters

Symbol	Description	Value
Systemic Circulation		
$R1$	Systemic vascular resistance	$0.6667 - 2.6667 \times 10^{-4} [kPa.sec/mm^3]$
$R2$	TAH inlet valve resistance	$6.6661 \times 10^{-7} [kPa.sec/mm^3]$
$R3$	TAH outlet valve resistance	$1.3332 \times 10^{-7} [kPa.sec/mm^3]$
$R4$	Characteristic resistance	$5.3062 \times 10^{-6} [kPa.sec/mm^3]$
$C2$	Left atrial compliance	$3.3003 \times 10^{4} [mm^3/kPa]$
$C3$	Systemic compliance	$9.9758 \times 10^{3} [mm^3/kPa]$
$C4$	Aortic compliance	$6.0005 \times 10^{3} [mm^3/kPa]$
I	Inertance of blood in Aorta	$6.6661 \times 10^{2} [kPa.sec^2/mm^3]$
HR	Heart beat frequency	$75 [bpm]$
Hydraulic Based TAH		
A_{mem}	Effective surface area of membrane	$2.83 \times 10^{-3} [m^2]$
C_{mem}	Reciprocal of membrane spring stiffness	$10^{-2} - 10^{-1}$
I_{mem}	Membrane mass	$5 \times 10^{-2} [kg]$
R_{mem}	Membrane damping	$1 - 10 [mN.sec/mm]$
B	Rotary damping of Motor+Pump	$50 - 500 \times 10^{-7} [kg.m^2/sec]$
D	Gear Pump Displacement	$50 \times 10^{3} [mm^3]$
J	Moment of Inertia of Motor+Pump	$50 - 200 \times 10^{-7} [kg.m^2]$
Pneumatic Based TAH		
A_{mem}	Membrane surface area	$2.8274 \times 10^{3} [mm^2]$
I_{mem}	Membrane mass	$5 \times 10^{-2} [kg]$
C_{mem}	Membrane spring stiffness	$10 - 100 [mN/mm]$
R_{mem}	Membrane damping	$1 - 10 [mN.sec/mm]$
V_{max}	Total chamber volume	$70 \times 10^{3} [mm^3]$

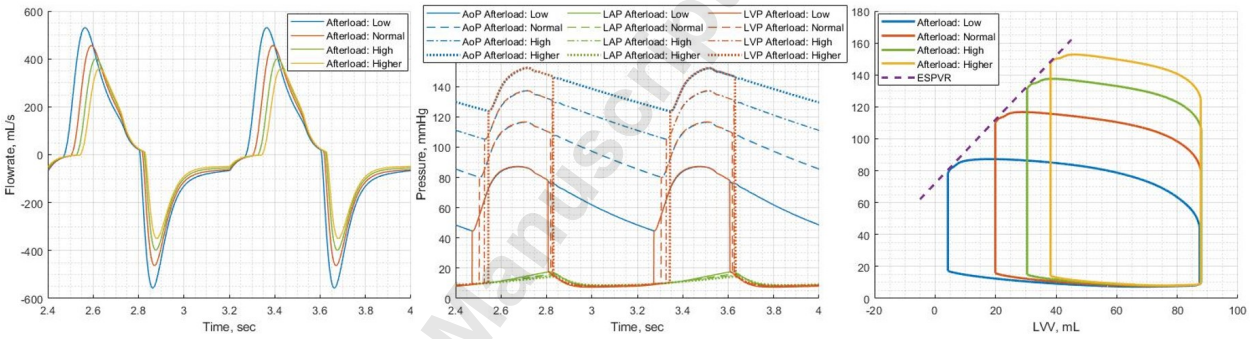

Fig. 4. (a) Flowrate vs time (b) Pressure vs time (c) PV-loops of the hydraulic based TAH with different afterload

Table 2. Hemodynamic parameters for the hydraulic based TAH with different afterload

Afterload $[mmHg.sec/mL]$	SV$[mL]$	CO$[LPM]$	AoP$[mmHg]$ $sys/dia/mean$	LAP$[mmHg]$ $max/min/mean$
0.5	83.82	6.2867	87.07/44.58/67.21	17.63/7.99/11.08
1.0	68.19	5.1143	116.52/77.99/99.35	16.19/8.32/10.98
1.5	57.59	4.3193	137.24/105.16/121.92	15.31/8.54/10.88
2.0	50.01	3.7508	152.33/123.62/138.41	14.58/8.65/10.72

[6] Ferreira, A., Chen, S., Simaan, M. A., Boston, J. R., and Antaki, J. F., 2005. "A nonlinear state-space model of a combined cardiovascular system and a rotary pump". In Proceedings of the 44th IEEE Conference on Decision and Control, IEEE, pp. 897–902.

[7] Simaan, M. A., Ferreira, A., Chen, S., Antaki, J. F., and Galati, D. G., 2008. "A dynamical state space representation and performance analysis of a feedback-controlled rotary left ventricular assist device". *IEEE Transactions on Control Systems Technology,* **17**(1), pp. 15–28.

[8] Santamore, W. P., and Burkhoff, D., 1991. "Hemodynamic consequences of ventricular interaction as assessed by model analysis". *American Journal of*

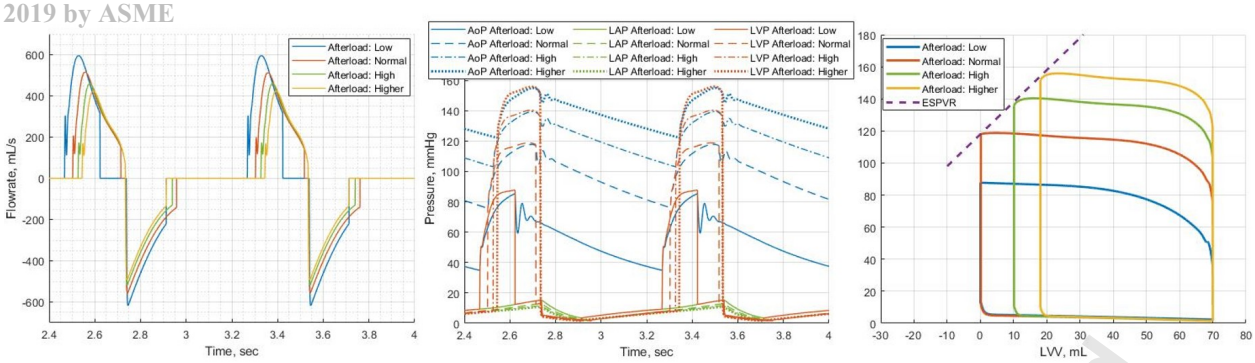

Fig. 5. (a) Flowrate vs time (b) Pressure vs time (c) PV-loops of the pneumatic based TAH with different afterload

Table 3. Hemodynamic parameters for the pneumatic based TAH with different afterload

Afterload $[mmHg.sec/mL]$	SV$[mL]$	CO$[LPM]$	AoP$[mmHg]$ $sys/dia/mean$	LAP$[mmHg]$ $max/min/mean$
0.5	70	5.2500	85.31/34.87/56.07	15.36/3.51/8.84
1.0	70	5.2500	117.86/75.72/97.41	13.15/2.07/7.02
1.5	59.94	4.4955	139.40/103.03/121.78	11.75/1.91/6.42
2.0	52.03	3.9022	155.06/122.18/138.72	10.92/1.95/6.18

Physiology-Heart and Circulatory Physiology, **260**(1), pp. H146–H157.

[9] Klute, G., Tasch, U., and Geselowitz, D., 1992. "An optimal controller for an electric ventricular-assist device: Theory, implementation, and testing". *IEEE transactions on biomedical engineering,* **39**(4), pp. 394–403.

[10] Tsach, U., Geselowitz, D., Sinha, A., and Hsu, H., 1989. "A novel output feedback pusher plate controller for the penn state electric ventricular assist device". *Journal of dynamic systems, measurement, and control,* **111**(1), pp. 69–74.

[11] Slepian, M. J., Alemu, Y., Soares, J. S., Smith, R. G., Einav, S., and Bluestein, D., 2013. "The syncardia™ total artificial heart: in vivo, in vitro, and computational modeling studies". *Journal of biomechanics,* **46**(2), pp. 266–275.

[12] Mohacsi, P., and Leprince, P., 2014. The carmat total artificial heart.

[13] Lankhaar, J.-W., Rövekamp, F. A., Steendijk, P., Faes, T. J., Westerhof, B. E., Kind, T., Vonk-Noordegraaf, A., and Westerhof, N., 2009. "Modeling the instantaneous pressure–volume relation of the left ventricle: a comparison of six models". *Annals of biomedical engineering,* **37**(9), pp. 1710–1726.

[14] Yu, Y.-C., Boston, J. R., Simaan, M. A., and Antaki, J. F., 1998. "Estimation of systemic vascular bed parameters for artificial heart control". *IEEE Transactions on Automatic Control,* **43**(6), pp. 765–778.